

## STUDIES ON THE PHOTOELECTRON CLOUD AT THE BEPC\*

Z.Y. Guo, Q. Qin, J.S. Cao, H. Huang, L. Ma, J.Q. Wang, J. Xing, G. Xu, C. Zhang, Z. Zhao, Institute of High Energy Physics, Chinese Academy of Sciences, Beijing, 100039, P.R. China, K.C. Harkay, Argonne National Laboratory, Argonne, IL 60439, USA, H. Fukuma, E. Kikutani, M. Tejima, High Energy Accelerator Research Organization, 1-1Oho, Tsukuba, Ibaraki, 305, Japan

### 1 INTRODUCTION

Many experiments on photoelectron instability (PEI) have been carried out at the Beijing Electron Positron Collider (BEPC) in IHEP, China, in collaboration with KEK[1]. Based on the detectors at Advanced Photon Source (APS), ANL, a specially-constructed detector was installed in the BEPC. It is hoped to obtain realistic values for the photoelectron (PE) and secondary electron yields as well as the energy spectrum of the electron cloud through the direct measurements of the properties of the PE cloud for both stable and unstable beams. In this paper, the experimental results at the BEPC are presented after the description of the instrumentation, and some results of simulation and discussions are followed afterwards.

### 2 INSTRUMENTATION

#### 2.1 PE detector

Similar to the detector in the APS[2,3], a photoelectron detector was installed in the BEPC ring. It has three layers with the same diameter of 80 mm and two mesh grids in front of the detector. The outermost grid is grounded, and a bias voltage is applied to the shielded grid. The graphite-coated collector lowers the secondary electron yield and is biased with a DC voltage of +48 V with batteries. Between the detector and the support barrel mounted on an idle slot, a 1 cm annular gap exists.

The detector is mounted downstream of a dipole in the direction of positron motion, shown in Fig. 1, with a distance of 230 mm between the dipole and the detector.

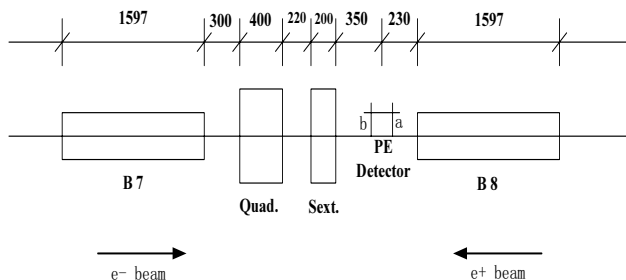


Figure 1: Position of the PE detector at the BEPC storage ring (seen from inside of the ring).

Being so close to the dipole, the PE detector has to be shielded from the magnetic field with layers of high and low permeability “mu-metal” sheets and nickel alloy sheets. After shielding, the fields at the points *a* and *b* in

Fig. 1 are 9 Gauss and 0, respectively. At the centre inside the detector chamber, the fringe field of the dipole is measured using a model chamber installed in a reference dipole, which has the same field of the dipoles in the storage ring. The result confirms the effect of shielding.

#### 2.2 Apparatus setup

The detector is connected with other instruments as shown in Fig. 2. A low pass filter (LPF) is used to make sure that the signal of collector is from the electron only. A 0.1MΩ resistor checks the direction of the current from the collector, associated with the voltmeter. The current of photoelectron is measured with the nanoammeter, which is connected between the resistor and ground. It can also cross-check the readings of the voltmeter. A temperature monitor is mounted on the detector to detect heat induced by beam-excited HOM wakefields in the annular gap between the detector and the support barrel.

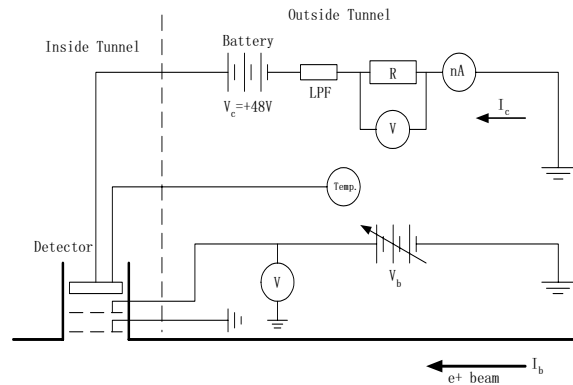


Figure 2: Setup of all apparatus in the experiment.

### 3 MEASUREMENTS

#### 3.1 Instrumentation check with beam

The LPF filters beam-induced RF noises. The detector current ( $I_c$ ) is measured as a function of beam current for LPFs with different cutoff frequencies, shown as Fig. 3. In the following PE measurements, we apply the 150 MHz LPF to eliminate any sources of RF noise. During all the measurement, the temperature monitor displays  $24 \pm 1^\circ\text{C}$  with no change, which means the HOMs effect due to the annular gap between the detector and its support barrel is minimal. All these confirm the validity of the whole measurement system.

A bias voltage scan was made and the  $V_b$  fixed at +40V for maximum signal, as shown in Fig. 4. It can be seen that electron beam creates a PE signal 6 times lower than

\*Work supported by the Chinese National Foundation of Natural Sciences, contracts 19875063-A050501 and 19975056-A050501

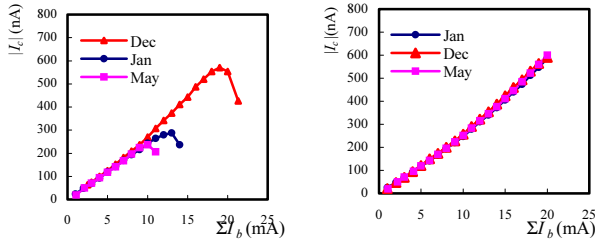


Figure 3: Effect of LPF.

(Left: without LPF, Right: with 150 MHz LPF)

the positron beam. One explanation is that the detector is located 6 times closer to the downstream dipole (B8) for the positron beam, than the distance from the detector to the downstream dipole (B7) for the electron beam, shown in Fig. 1. Another reason may be that the interaction of the PE with the positron beam may cause more electrons to be deflected into the detector. So positron beam is used in the following measurements.

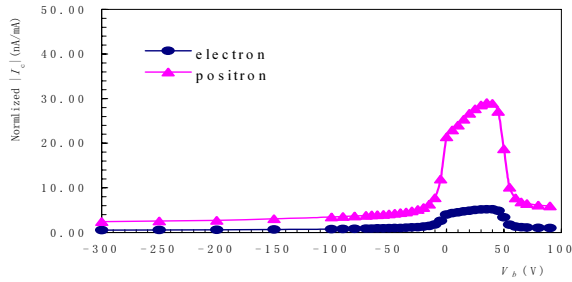


Figure 4: Detector current when bias voltage scans.

### 3.2 Dependence on beam current

The collected electron current  $I_c$  as a function of beam current  $I_b$  is measured in the cases of single bunch and multi-bunch. Normalized by  $I_b$ ,  $I_c$  is almost the same in different bunch spacing. It reads about 25nA/mA at the bunch current of 2 mA, similar to the right plot of Fig. 3.

No any saturation effect, in which electron generation and loss equilibrate, is found with a long bunch train and a weak bunch current, even 40 bunches are used with the bunch current of 1 or 2 mA ( $I_b$  is 40 or 80 mA). The reason might come from the fact that the detector is located very near the dipole and there is no antechamber, causing the primary photoelectron emission to dominate over secondary electron emission.

The derivative of the normalized  $I_c$ - $V_b$  curve gives the photoelectron energy distribution, shown as Fig. 5.

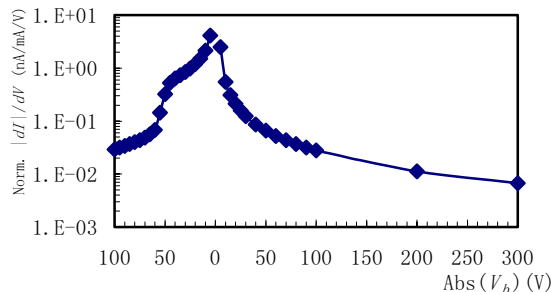


Figure 5: Photoelectron energy distribution.

### 3.3 Secondary electron (SE) measurement

Due to the SE, a dramatic amplification of the signal is observed in the APS when the bunch spacing is 7 buckets (20 ns) [2]. The energy gain of the electrons kicked by the beam is determined by  $\Delta p = 2m_e N_b r_e c/a$ , where  $a$  is the radial distance from the beam and  $r_e$  the classical electron radius. The beam-induced multipacting may be expected to appear on 5-bucket spacing and 6 mA/bunch in the BEPC, compared with the APS. But in our measurements, such an amplification is not observed when the bunch spacing and current are scanned from 1 mA/bunch to 6 mA/bunch with the bunch spacing from 1 to 12 buckets in a bunch train of 5 and 10 bunches, shown in Fig. 6. The only result is the normalized electron current increases when the bunch current increases. The reason may come from the short distance between the bending magnet and the detector, which may cause the photoelectrons to dominate and possibly suppress the secondary electrons.

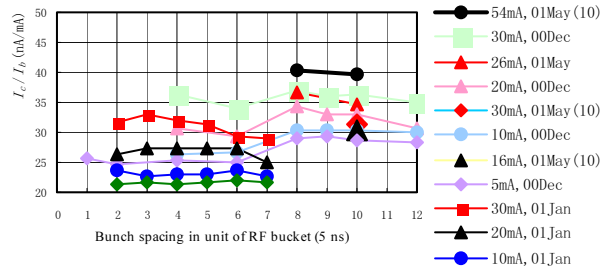


Figure 6: Normalized electron current as a function of bunch spacing and current. The legend gives beam current.

### 3.4 Dependence on beam parameters

We measure the  $I_c$  as functions of beam parameters, too. The correlations were measured with the different closed orbits, beam energies, beam emittances and chromaticities, respectively. The PE distribution is quite sensitive to the beam position, since  $I_c$  has 1nA linear increment when the vertical closed orbit increases 1mm with an  $I_b$  of 1mA. The dependences of  $I_c$  on beam energy, emittance and chromaticity are not sensitive when the closed orbit fixes.

A kind of vertical coupled-bunch instability occurs and a broad spectrum appears for the positron beam when the threshold beam current of 9.7 mA is reached. We set the beam conditions as the total beam current of 9.8 mA with 160 bunches uniformly distributed around the storage ring in each bucket, the beam instability occurs as before. The  $I_c$  is then measured in the cases of stable and unstable beams. The relations of  $I_c$  vs.  $I_b$  and normalized  $I_c$  vs.  $V_b$  have the same regulations for both stable and unstable beams. The instability is also observed with 16.6 mA in 116 bunches, and the  $I_c$  dependence is the same as the stable case. This indicates the beam oscillation due to PEI does not influence the yield of the photoelectron.

### 3.5 Solenoid effect

Solenoid coils winding downstream the dipoles is a possible way to cure the PEI, like KEKB LER. In BEPC storage ring, we installed two coils on each side of the

detector to observe the solenoid effect. The currents of the coils,  $I_s$ , are  $\pm 20A$ , generating several tens of Gauss magnetic field. Fig. 7 shows the  $I_c$  vs.  $I_b$  when solenoid has different currents. When we scan the bias voltage  $V_b$ ,  $I_c$  is given in Fig. 8.

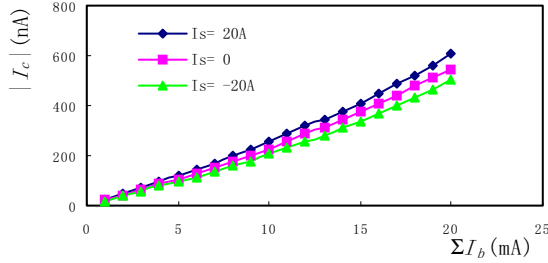


Figure 7:  $I_c$  vs.  $I_b$  with different solenoid fields.

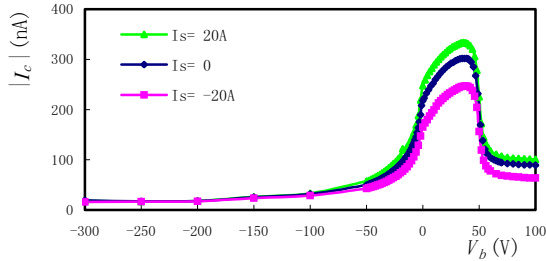


Figure 8:  $I_c$  vs.  $V_b$  with different solenoid fields.

It can be seen that the solenoid field does influence the electron cloud, but it is not a strong effect. The difference when the direction of the solenoid field changes comes from the combining effect of the solenoid field and the fringe field of the dipole, which locates near the detector. The combined field was also measured in the same way as the fringe field measurement described previously.

## 4 SIMULATIONS

With the code developed by Dr. Y. Luo [4], the PE generation is simulated for different PE reflectivity. For a real machine, a reflectivity of 0.98 is chosen in simulation. The energy distribution of the PE is selected as  $5eV \pm 5eV$ . The emission yield of secondary electron is given as

$$\delta(E, \theta) = \delta_{\max} \cdot 1.11 \cdot \left(\frac{E}{E_{\max}}\right)^{-0.35} \cdot \left(1 - \exp\left[-23 \cdot \left(\frac{E}{E_{\max}}\right)^{1.35}\right]\right) / \cos \theta$$

with  $\cos \theta$  distribution as the angle distribution.

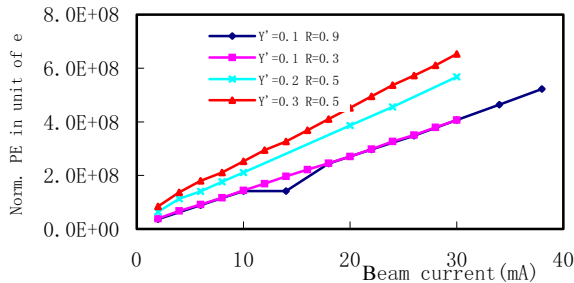


Figure 9: PE creation for different yield and reflectivity. The energy distribution of the SE is  $0 \pm 5eV$ , and the  $\delta_{\max}$  of the SE is 3 in simulation. Simulation results are shown in Fig. 9 and 10.

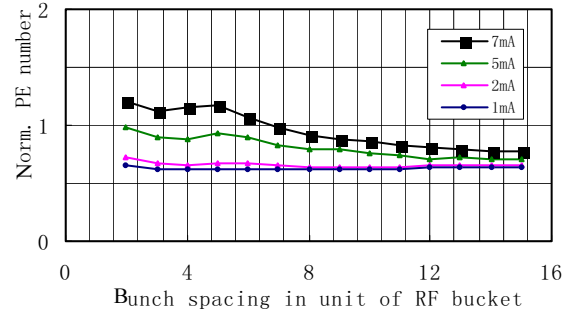


Figure 10: Simulation results on multipacting. (The legend gives bunch current.)

## 5 DISCUSSIONS

Detailed measurements of the properties of PE cloud were carried out at the BEPC storage ring under various beam conditions. Comparisons were made between single and multi-bunch cases as well as for positron and electron beams.  $I_c$  varies linearly with the beam current  $I_b$  as expected, since the photoelectron number is proportional to the photon intensity and the beam current. This is the same behaviour for single bunch and a number of multi-bunch patterns. No saturation process is observed up to 40 bunches with 1 or 2 mA/bunch. We observed very weak dependence on bunch spacing, using 5 and 10 bunches with 1 to 6 mA/bunch up to the 12-bucket spacing. No beam-induced multipacting was observed at the BEPC yet. No significant differences were observed in  $I_c$  behaviours for stable and unstable beams.

The distance between detector and dipole influences the measurement of SE and the saturation process very much. Two new detectors, modified as encircling the grounded grid but isolated from the retarding grid and the collector to avoid the  $I_c$  electrical leak from HOMs excited through the gap between the detector and the port, will be installed soon in the places far from dipoles. The time structure of  $I_c$  signal and the machine parameter dependences would be studied furthermore. Better shielding is necessary on the existing detector to avoid the fringe field of the dipole.

Primary simulations give some consistent results with the experiments, especially the multipacting condition and the dependences of beam parameters. More simulation studies are still under way.

## 6 ACKNOWLEDGEMENTS

We wish to thank the BEPC team for their effective work on operating the machine during the experiment. The authors would also like to thank Dr. R. Rosenberg from ANL, for his suggestion on shielding the detector.

## 7 REFERENCES

- [1] Z.Y. Guo, et al, Proc. of PAC'97, 1997, EPAC'98, APAC'98, 1998.
- [2] K. Harkay, R. Rosenberg, Proc. of PAC'99, 1999.
- [3] R. Rosenberg, K. Harkay, NIM A 453 (2000) 507.
- [4] Y. Luo, IHEP Ph.D dissertation, 2000.